






## Original Article


## Morphologic changes of simple star dunes during the growth process in Dunhuang, China


AN Zhi-shan<sup>1,2,3</sup>  <https://orcid.org/0000-0003-0262-4717>; e-mail: an1986wen@163.com

ZHANG Ke-cun<sup>1,2\*</sup>  <https://orcid.org/0000-0003-3270-2843>;  e-mail: kecunzh@lzb.ac.cn

TAN Li-hai<sup>1,2</sup>  <https://orcid.org/0000-0001-7727-9722>; e-mail: tanlihai18@163.com

NIU Qing-he<sup>1,2</sup>  <https://orcid.org/0000-0002-7600-3502>; e-mail: niuqh@lzb.ac.cn

LIU Ben-li<sup>1,2</sup>  <https://orcid.org/0000-0002-7664-5142>; e-mail: liubenli@lzb.ac.cn

NIU Bai-cheng<sup>1,2</sup>  <https://orcid.org/0000-0002-4962-5998>; e-mail: 707481314@qq.com

\*Corresponding author

<sup>1</sup> Dunhuang Gobi and Desert Research Station, Northwest Institute of Eco-Environment and Resources, Chinese Academy of Sciences, Lanzhou 730000, China

<sup>2</sup> Key Laboratory of Desert and Desertification, Chinese Academy of Sciences, Lanzhou 730000, China

<sup>3</sup> University of Chinese Academy of Sciences, Beijing 100049, China

**Citation:** An ZS, Zhang KC, Tan LH, et al. (2022) Morphologic changes of simple star dunes during the growth process in Dunhuang, China. *Journal of Mountain Science* 19(4). <https://doi.org/10.1007/s11629-021-6970-5>

© Science Press, Institute of Mountain Hazards and Environment, CAS and Springer-Verlag GmbH Germany, part of Springer Nature 2022

**Abstract:** Star dune is one typical kind of aeolian geomorphology in global sand seas. It has attracted scholars in various research fields for years because of its unique morphologic features like Egyptian pyramid. The landform pattern of star dune is mainly dominated by factors such as regional wind regime, sand availability, and local topography. Star dunes grow vertically as they accumulate sand brought in from different directions; however, little is known regarding morphologic changes during this process. The stability of star dunes based on quantitative data is another unsolved question due to the limitation in measuring equipment or other factors. And whether the star dune can grow into star sand hills is another scientific problem which needs to be discussed. In this paper, the heightening development process and morphological changes of star dunes were monitored

in Mingsha Mountain of Dunhuang with the 3D laser scanner. Results show that the star dunes in Mingsha Mountain were formed by a group of relatively steady winds, which were northwest, northeast and south winds. With the increase of the height of the star dunes, the morphological parameters of the dune, such as the volume and bottom area, did not show regular changes. The surface erosion of both Dune 1 and Dune 2 during the observation period was closely related to the regional wind conditions. During the growth of the star dunes, the overall trend of the dunes was relatively steady and the dune shape maintained its stability although the aspect and slope of the sand dunes changed, indicating that the stability of star dune was not complete and was dynamic. Moreover, the variation range of the dune slope was proportional to the volume change of the dune.

**Received:** 23-Jun-2021

**1<sup>st</sup> Revision:** 10-Nov-2021

**2<sup>nd</sup> Revision:** 16-Dec-2021

**Accepted:** 14-Jan-2022

**Keywords:** Star dune; 3D laser scanner; Dunhuang; Morphologic change

## 1 Introduction

In the world's sand-sea area, star dunes are the tallest sand dunes, which are classified as composite type with a unique, steady and less movable shape. Its pattern is dominated by heightening and balanced development, which is affected by wind direction, sand source, topography, and atmospheric boundary layer (Andreotti et al. 2002; Rubin et al. 2008; Ulrike 1999; Wasson et al. 1984). Star dunes grow vertically as they accumulate sand brought in from different directions (Lancaster 2010; Lancaster 1989; Zhang et al. 2000; Zhang et al. 2016). The movement of star dunes was different from those of transverse and longitudinal sand dunes (Breed et al. 1979; Qu et al. 1992; Zhang et al. 2000; Wang et al. 2005). Based on the combination of its morphological features, Breed and Grow (1979) categorized star dunes into simple and composite star dunes, which could also be divided into rudimentary and large mature star dunes according to its formation stage. Rudimentary star dunes that are subjected to strong winds for a long time easily lose their basic morphological features and evolve into other forms of sand dunes. Large mature star dunes are large in scale and have typical pyramid characteristics that retain even if they are subjected to strong winds for a long time (Breed et al. 1979).

For a long time, researchers have used field observations, wind tunnel experiments, and numerical simulations to investigate the formation and development of star dunes and to determine the various developmental patterns of star dunes. For example, Bagnold (1941) discovered that star dunes formed before mountains and that airflow was blocked by the mountains, such that the return airflow interfered with the original airflow and convective updraft played an important role. Zhu (1981) found that the formation and development conditions of star dunes included multi-directional winds and ups and downs in the underlying terrain along with residual hills and terraced areas. Xu (1983) believed that the interference of air movements in the mountains caused multi-directional and balanced winds, which had important effect on the formation of star dunes. Qu (1992) indicated that star dunes formed downwards by three groups of winds and reproduced the formation process in the wind tunnel experiments. In recent years, with the maturity of numerical simulation technology and the use of observation equipment, the complex flow field

structure of the star dune surface has been revealed (Breed et al. 1979; Zhang et al. 2012; Blocken et al. 2015). For instance, the results of Tan (2016) showed that incident flow conditions (longitudinal or transverse airflow) controlled by the angle between incident flow and dune ridgeline exert a considerable effect on wind flow patterns over star dunes. Zhang (2016) had shown that airflow stagnation and deflection caused by topography were the major mechanisms for the formation of star dunes. Andreotti (2009) showed that giant aeolian dune size was determined by the average depth of the atmospheric boundary layer.

The previous researches have verified the various formation and development patterns of star dunes and indicated that star dunes were dominated by high and balanced development and grow vertically (Zhang et al. 2000; Zhang et al. 2012; Zhang et al. 2016; An et al. 2018; Andreotti et al. 2009). But two problems remain on account of measuring equipment or other factors. The first problem is morphologic changes of star dunes during the vertically increasing process. The second problem is how to define the stability of star dunes in different formation stages. And whether the star dune can grow into star sand hills is another scientific question which needs to be resolved. Although it proves that the star dune shape is steady and less movable, it is mostly based on morphological analysis without enough quantitative data. The reason is that the previous equipment, such as total station, only obtains a single point data every time and has to spend a long time to measure the whole dune (An et al. 2016). The accuracy grade of aerial photo can not fully meet data requirements (Zhang et al. 2000). Thus, previous research mainly focuses on the formation and change of sand dunes on a two-dimensional scale, while those on the changes in the three-dimensional shape of sand dunes, such as morphological parameters of slope direction and angle are still relatively weak.

As a high-tech product, 3D laser scanners have been successfully applied in many fields such as cultural relics protection, urban building surveying, topographic surveying, highway and railway construction, and many other fields ( Hanke et al. 2015; Isa et al. 2017; Leng et al. 2006; Zhu et al. 1981). The 3D laser scanner can directly obtain the spatial point cloud information and construct the complex and irregular 3D visualization model, which can save much time. The measurement data include not only X,

Y, Z information, but also R, G, B color and other information. Compared with the two-dimensional results obtained by traditional measurement methods, its advantage is huge. To date the 3D laser scanning technology has gradually become one of the indispensable technical means in surveying. In the study of aeolian geomorphology, 3D laser scanners have gradually begun to be applied (An et al. 2018).

In view of this, this study used a 3D laser scanner, which had a rate of  $1,000,000 \text{ pt}\cdot\text{s}^{-1}$  and measurement distance between 580 m and 2,050 m, to monitor the typical star dunes in Mingsha Mountain of Dunhuang and analyzed morphological changes of star dunes during vertically increasing process, and tried to define the stability of star dunes quantitatively.

## 2 Study Area

The Mingsha Mountain extends from southwest to northeast for approximately 40 km with a width of 15 km and is located approximately 5 km south of Dunhuang City, which is a well-known historical and cultural city in Gansu Province, China. Within such a range, tall and compound mega star dune are widely distributed (Fig. 1).

Dune 1 is a three-armed star dune with a relative height of 4.6 m. Its three arms extend to the directions of northwest ( $10^\circ$ ), southeast ( $130^\circ$ ), and

southwest ( $225^\circ$ ). The lengths of the arms are 18.3, 32, and 31.8 m. Moreover, there are three faces between every two adjacent sand arms, which are the NW, NE and S slope faces. The ratio of the three slope faces is relatively balanced and has no significant difference. The lengths of the slope faces are 10.1, 10.7 and 18.3 m from the top to the bottom of every face. The west and northeast slope faces are slightly steep, showing a typical slip surface, and the northwest slope is slightly low. Dune 2 is located on the east of Dune 1, with the distance of 200 m. The relative height is approximately 5 m. Its three arms extend to the northwest ( $30^\circ$ ), east ( $90^\circ$ ), and southwest ( $205^\circ$ ) directions. Among the three arms, the southwest arm has the longest length of 36.2 m, and the northwest and east arms are 15 and 19.7 m, respectively. Moreover, there are three slope faces between every two slope faces, which are the W, NE and SE slope faces. Of the three slopes, the W and SE slope faces are slightly larger than the NE slope face. The area percent of the W and SE slope face is approximately 35%, whereas that of the NE slope face is approximately 30%. The slope lengths are 9, 17 and 8.7 m. The west and southeast slopes are slightly steep, showing a slip surface, and the northeast slope is slightly low.

## 3 Methods

The application possibilities of 3D laser scanning methods under polar conditions were tested using the RIEGL VZ2000 scanner. The operation of the scanner model tested is based on stationary laser distance measurements with a rate of  $1,000,000 \text{ pt}\cdot\text{s}^{-1}$ . The scanning geometry of the RIEGL VZ2000 scanner (i.e. up to  $360^\circ$  horizontally and up to  $100^\circ$  vertically) enables measurements in almost any terrain condition. The measured distance is between 580 m and 2050 m (Fig. 2b).

Topographic data acquisition can be divided into two parts, namely, field operations and indoor work. Specifically, the time of field operations were in November 2015, April 2016 and November 2016 to lay out the control points and obtain data. Firstly, not only the control points were laid out but also a local coordinate system was established within the survey region to guarantee that the scanned data were within an identical coordinate system through the GPS RTK. Secondly, the 3D laser scanner was used to conduct



**Fig. 1** Location map of the study area and the monitored star dunes (The picture is from Google Earth).

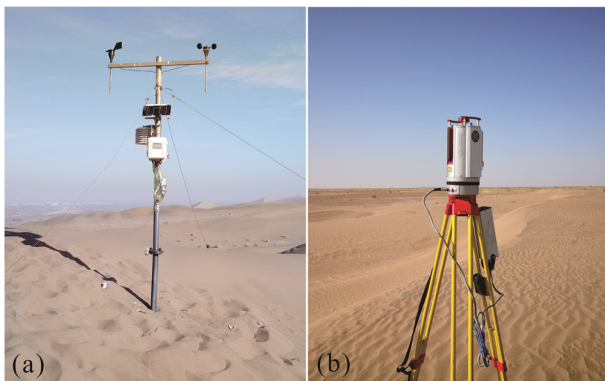


**Fig. 2** Observation instruments. (a) HOBO U30 weather station; (b) RIEGL VZ2000 3D laser scanner.

multi-station scanning of the survey region. Specifically, the density of the scanned data set was 7 cm × 7 cm in 100 m.

The principal indoor work involves the post-processing of data, which includes the combination, optimization and extraction of point cloud data. The first step is to open the original scanned data of each station and check whether the data covered the required terrain completely. The second step is to check the coordinates of each scanning station and conduct the multi-site splicing according to the GPS RTK of each target piece. The third step is to optimize the data. Data optimization refers to the elimination of point cloud data irrelevant to the research object, as well as point cloud integration and simplification. By removing the error points from the original point cloud data, the initial characteristics of the research object can be restored to improve the signal-to-noise ratio of the data. The fourth step is to check the corresponding error. If the corresponding error is more than 6 mm, then we should process the data again.

After implementing the previous steps, we exported the selected point cloud data, including the x, y and z, to text file, with precision higher than 6 mm. We opened the text file using ArcGIS 10.2 to show all the points on the screen. The final step is to create the raster data model and calculate the height, basal area, and volume of dunes.

To calculate the dune volume, an elevation of 0 m was used as the reference base level. And the area of the base level is defined as the basal area and the edge of dune. The elevations of the two dunes reference base level are the same. The height of the dune is defined as the highest point above the base level.

A HOBO U30 weather station was set up in the study area to measure the wind speed and direction

(Fig. 2a). It was on the top of Dune 1, which was the highest point in the study area. Around the meteorological instrument were the sand dunes. The surrounding vegetation coverage was low. The kind of vegetation type was mainly *Nitraria tangutorum* Bobr). The height of the wind speed and wind direction sensors was 2 m above the ground. The data acquisition time interval was 10 min. Sand Drift Potential (DP) was calculated using the following transport equation (Fryberger et al. 1979):

$$DP = V^2 \times (V - Vt) \times t \quad (1)$$

where DP is the sand drift potential expressed in vector units (VU). Wind speed,  $V$ , is greater than the value of sand-moving wind.  $Vt$  is the threshold wind speed for sand-moving ( $Vt=5 \text{ m}\cdot\text{s}^{-1}$ ).  $t$  is the time affected by sand-moving wind (unit: min).

## 4 Results

### 4.1 Sand drift potential

From 2015 to 2017 (Fig. 3), three distinct wind directions were observed in the region, namely, the northwest, northeast and south winds. Among them, the annual sand DP was 231.45 VU in 2015, the resultant sand DP was 74.47 VU, the resultant drift direction was 39.64° and the direction variability was 0.32, which was the ratio of the resultant sand DP to the sand DP. In 2016, the annual sand DP was 474.95 VU, the resultant sand DP was 73.92 VU, the resultant drift direction was 70.09°, and the direction variability was 0.16. In 2017, the sand DP was 285.74 VU, the resultant sand DP was 9.96 VU, the resultant drift direction was 215.96°, and the direction variability was 0.03. Although the three groups of winds had slightly different sand transport potentials during every year, the wind direction was basically steady and the resultant sand DP was close. This finding indicated that star dunes were formed by a group of steady winds.

### 4.2 Morphological characteristics

During the period from November 2015 and November 2016, the heights of both Dune 1 and Dune 2 increased (Table 1). The height of Dune 1 increased from 4.3 m to 5.07 m, and the height increased by 0.77 m. The movement distance of the center of gravity of sand dune was 0.63 m. The height of Dune 2 increased from 4.46 m to 4.7 m, and the height

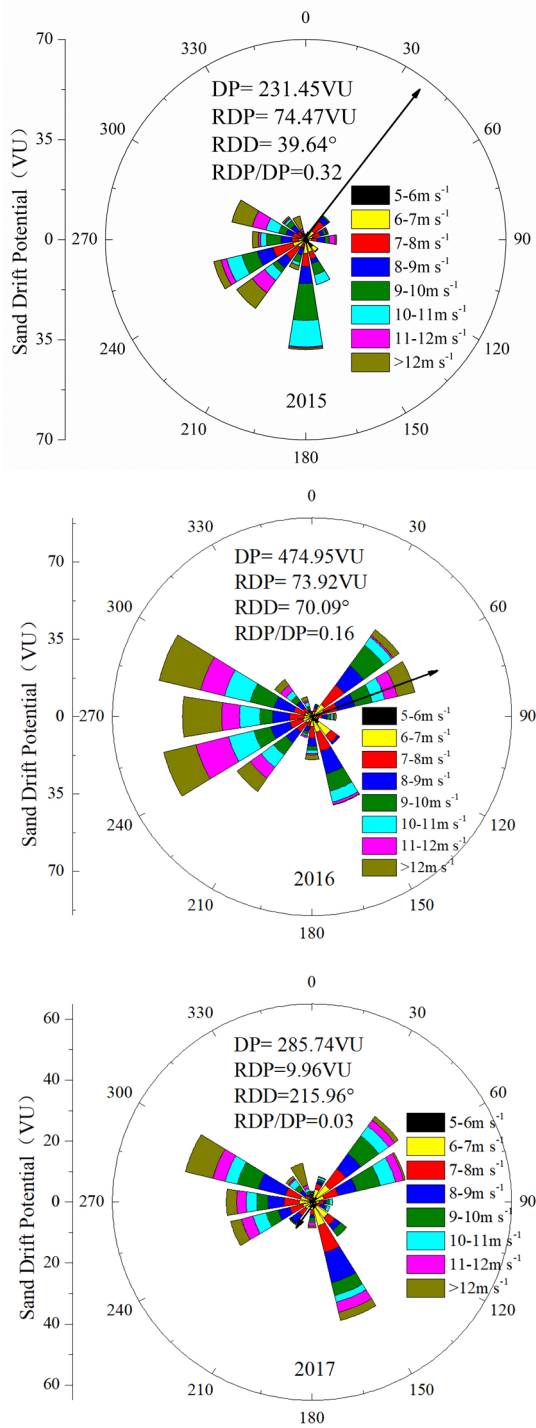


**Fig. 3** Rose of sand drift potential during 2015-2017. RDP means Resultant Drift Potential (unit: VU). DP means Drift Potential (unit: VU).

increased by 0.24 m, which was less than that of Dune 1. And the movement distance of the gravity center of sand dune was 0.24 m, which was also less than Dune 1. The analysis of the changes in sand dune morphological parameters showed that there was no

**Table 1** Morphological parameters of the star dune in different monitoring periods.

Sand dune	Period	Basal area (m <sup>2</sup> )	Superficial area (m <sup>2</sup> )	Vol.(m <sup>3</sup> )	Ht (m)
No.1	201511	1001.00	1074.62	1882.1	4.30
	201604	1024.24	1091.01	1828.23	4.84
	201611	980.06	1051.45	1892.64	5.07
No.2	201511	835.99	892.40	1370.54	4.46
	201604	873.69	935.43	1354.9	4.53
	201611	840.20	900.73	1422.58	4.70

obvious correlation between the variation of each parameter and the height of the sand dunes. Both the bottom and surface areas of Dune 1 and Dune 2 initially increased and subsequently decreased. However, the volumes of the star dunes showed a trend of initial decrease and subsequent increase.

The relationship between the direction and distance of sand dunes and the wind energy environment showed that the direction of sand dune movement was obviously related to the regional wind conditions. The direction of gravity of the dune was similar to that of the synthetic sediment transport potential. Moreover, the moving distance was proportional to the synthetic sediment transport potential. The larger the resultant sand DP was, the longer the moving distance. Furthermore, the moving distance was inversely proportional to the dune volume. The larger the dune volume was, the shorter the moving distance. Thus, wind condition was one of the main factors that affected the movement of sand dunes. Nevertheless, the volume of sand dunes, surrounding topography and vegetation also affected the movement of sand dunes.

### 4.3 Erosion and deposition

Based on previous observations, during the period from November to April of the following year, the prevailing wind direction in Dunhuang was the west and northwest wind. The period from November 2015 to April 2016 was selected as a typical wind season to analyze the wind erosion accumulation of star dune during wind seasons. As shown in Fig. 4, the sand DP was 166.46 VU during November 2015 to April 2016, the resultant sand DP was 26.48 VU, the resultant drift direction was 82.13°, and the direction variability was 0.16.

As shown in Fig. 5, during the period from November 2015 to April 2016, the sand dune volume decreased in both Dune 1 and Dune 2. The volume of

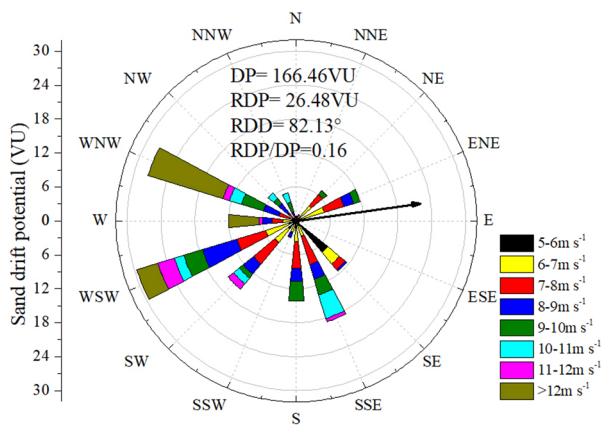


**Fig. 4** Rose of sand drift potential from November 2015 to April 2016.

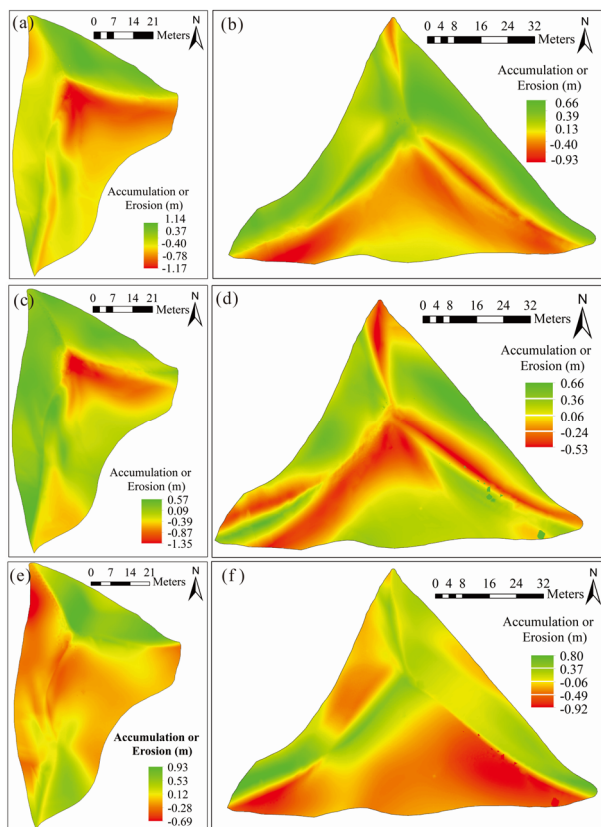


**Fig. 5** Dynamics of the monitored star dune in the three monitoring periods. (a) Dune 1, from November 2015 to April 2016; (b) Dune 2, from November 2015 to April 2016; (c) Dune 1, from April 2016 to November 2016; (d) Dune 2, from April 2016 to November 2016; (e) Dune 1, from November 2015 to November 2016; (f) Dune 2, from November 2015 to November 2016. When the value is positive (+), it represents accumulation; when the value is negative (-), it represents erosion.

Dune 1 decreased by 53.87 m<sup>3</sup>, whereas the volume of Dune 2 decreased by 15.64 m<sup>3</sup>. The surface erosion area of both Dune 1 and Dune 2 was larger than the

accumulation area. The proportion of the wind erosion area of Dune 1 was 55.71%, and the proportion of the accumulation area was 44.29%. The maximum wind erosion depth was 0.93 m, and the maximum accumulation thickness was 0.66 m. The proportion of the wind erosion area of Dune 2 was 51.87%, and the proportion of the accumulation area was 48.13%. The maximum wind erosion depth was 1.17 m, and the maximum accumulation thickness was 1.14 m. The analysis of the locations of wind erosion and accumulation showed that the wind erosion area of Dune 2 was mainly located on the south slope face, and the accumulation site was located on the northwest and northeast slope faces. Meanwhile, the wind erosion site of Dune 1 was mainly located on the southeast slope face and the accumulation site was located on the west and northeast slope faces. During the observation period, the sand-moving wind was dominated by the southeast, west, and northeast winds. Notably, the erosion status of star dunes was closely related to the wind conditions during this observation period. The southeast slope face of Dune 1 and the south slope face of Dune 2 were windward slopes. Thus, these slope faces showed the wind erosion status of star dunes. The other two slopes were stacked and leeward areas.

There were differences in terms of erosion and accumulation between the period from November 2015 to April 2016 and April 2016 to November 2016. Both Dune 1 and Dune 2 accumulated sand from April 2016 to November 2016, indicating that the dune volume increased. The volume of Dune 1 increased by 64.41 m<sup>3</sup> and the thickness per unit area was 0.07 m. Meanwhile, the volume of Dune 2 increased by 67.68 m<sup>3</sup> and the thickness per unit area was 0.1 m. The proportion of the wind erosion area of Dune 1 was 38.47%. The maximum wind erosion depth was 0.53 m and the average wind erosion depth was 0.21 m. The proportion of the accumulation area was 61.53%. The maximum accumulation thickness was 0.66 m and the average accumulation thickness was 0.24 m. The proportion of the wind erosion area of Dune 2 was 51.56%. The maximum wind erosion depth was 1.35 m and the average wind erosion depth was 0.4 m. The proportion of the accumulation area was 45.44%. The maximum accumulation thickness was 0.57 m and the average accumulation thickness was 0.25 m. The distribution area showed that the wind erosion area of Dune 1 was mainly concentrated near the sand ridgeline and on the upper part of the southeast slope

face. Both the northeast and west slope faces were stacked. Meanwhile, the wind erosion area of Dune 2 was mainly concentrated near the sand ridgeline. The other areas were stacked. In terms of the wind conditions from April 2016 to November 2016, the wind direction was still the northwest, northeast and southeast winds, which was consistent with the main wind directions during the typical wind season.

As shown in Fig. 6, the sand DP was 317.26 VU during April 2016 to November 2016, the resultant sand DP was 31.36 VU, the resultant drift direction was 117.8°, and the direction variability was 0.1. Combined with regional wind conditions, we found that its frequency was slightly lower and its speed was relatively slower than that of the typical wind season. This finding indicated that the regional wind energy environment was slightly low, and thus the sand dune movement was small, which was one of the main reasons for the accumulation from April 2016 to November 2016.

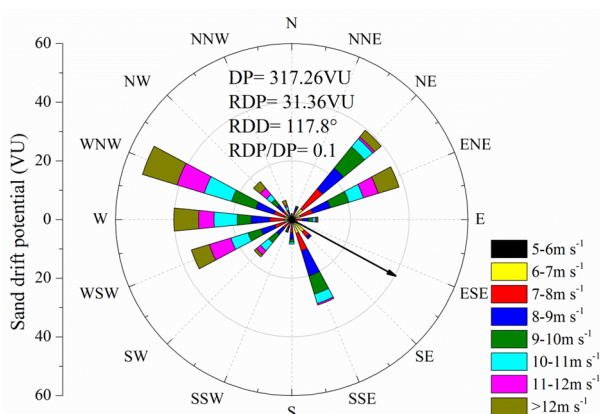


**Fig. 6** Rose of sand drift potential from April 2016 to November 2016.

From November 2015 to November 2016, the winds in the region were dominated by the southeast, northeast, and northwest winds. Moreover, the southeast and west winds had slightly higher frequencies than the northeast wind. Both Dune 1 and Dune 2 exhibited accumulation, and the volumes increased during the observation period (Fig. 5). The accumulation amount of Dune 1 was 10.54 m<sup>3</sup>, whereas the accumulation amount of Dune 2 was 52.04 m<sup>3</sup>. The average accumulation thickness of Dune 1 and Dune 2 was 0.08 m and 0.12 m, respectively. The proportion of the wind erosion area of Dune 1 was 61.69%, which was mainly distributed on the southeast and west slope faces. The maximum wind erosion depth was 0.92 m, and the average wind

erosion depth was 0.34 m. The proportion of the accumulation area was 38.31%, which was mainly located on the northeast slope face. The maximum stacking thickness was 0.8 m, and the average stacking thickness was 0.22 m. The proportion of the wind erosion area of Dune 2 was 50.36%, which was mainly distributed on the middle and lower parts of the south slope face and the lower part of the northwest slope face. The maximum wind erosion depth was 0.69 m, and the average wind erosion depth was 0.17 m. The proportion of the accumulation area was 49.64%, which was mainly located on the northeast slope face. The maximum stacking thickness was 0.93 m, and the average stacking thickness was 0.34 m. Notably, from 2015 to 2016, both for Dune 1 and Dune 2, the wind erosion area was mainly concentrated on the south and west faces. However, the northeast slope face had a large proportion of the deposition area. During the observation period, the frequencies of the southeast and west winds were slightly higher than those of the other winds. This finding is consistent with the wind conditions, wind erosion on the windward slope, and sand accumulation on the leeward slope.

#### 4.4 Dune aspect

According to Fig. 7, in periods of November 2015, April 2016, and November 2016, the dune aspect of Dune 1 was mainly northeast, southeast, and west, respectively, and the area proportion was 75.61%, 71.28% and 72.21%, respectively. The dune remained fairly steady, which was consistent with regional wind conditions. During the observation period, the southeast slope area was the largest, the west slope area was the second largest, and the northeast slope area was the smallest. The average area proportions of the slope faces during the observation period were 31.59%, 27.52% and 13.92%. The range of the slope area ratio from November 2015 to April 2016 showed that the proportion of the north, northeast, east, south, and northwest slope area increased. By contrast, the proportion of the other slope faces decreased, and the total area change rate was 9.33%. From April 2016 to November 2016, the proportion of the north, northeast and east slope faces decreased, whereas the proportion of the other slope faces increased. The total area change rate was 3.51%, which was smaller than that from November 2015 to April 2016. The area where the dune aspect changed

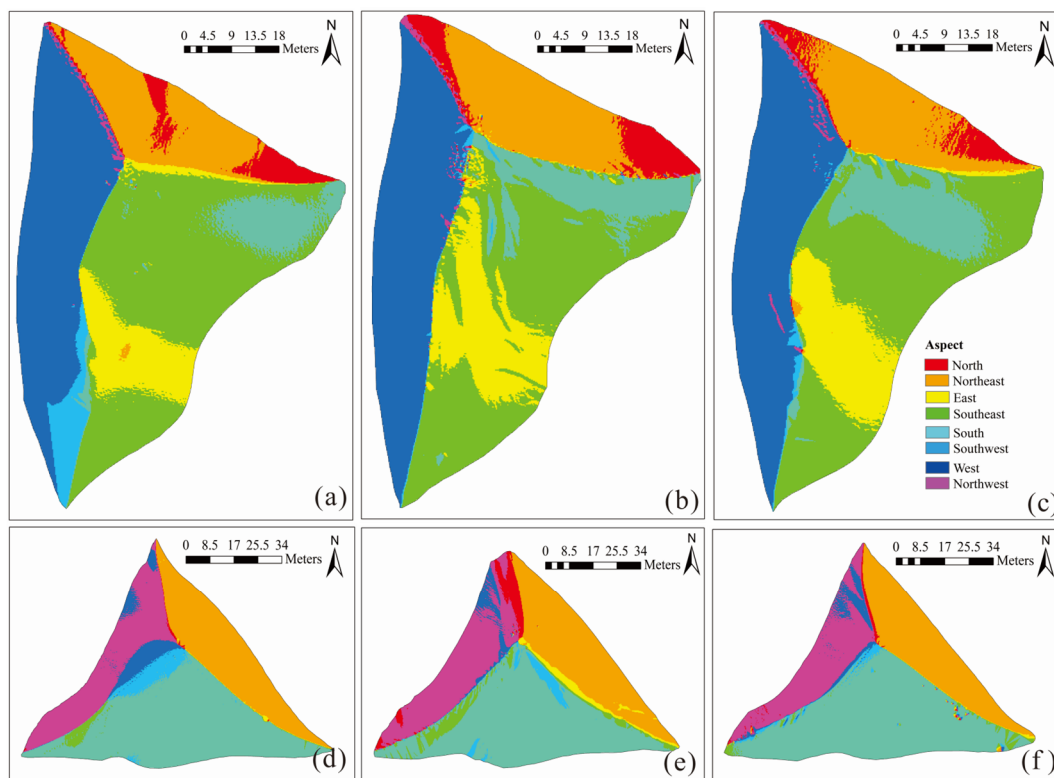


**Fig. 7** Slope aspect of the monitored star dune in the three monitoring periods. (a) Dune 1 in November 2015; (b) Dune 1 in April 2016; (c) Dune 1 in November 2016; (d) Dune 2 in November 2015; (e) Dune 2 in April 2016; (f) Dune 2 in November 2016.

was mainly located near the ridgeline, where the change of the dune aspect mainly occurred in the ridgeline movement process.

In November 2015, April 2016 and November 2016, the dune aspects of Dune 2 were mainly northeast, south and northwest, respectively, and the corresponding area proportions were approximately 87.94%, 84.33% and 91.15%, which were slightly larger than those of Dune 1. Among the three slope faces, the southward slope face was the largest, the northeast slope face was the second largest, and the northwest slope face was the smallest. The average proportions of the slope faces were 44.44%, 24.85% and 18.51%. From November 2015 to April 2016, the proportion of the north, northeast, east and southeast slope faces increased, whereas the proportion of the other slope faces decreased. The total area change rate was 8.13%. From April 2016 to November 2016, the proportion of the south and west slope faces increased, whereas the proportion of the other slope faces decreased. The total area change rate was 9.41%, which was greater than the former.

In summary, although the slope changed, the shape of both Dune 1 and Dune 2 remained basically steady during the growth process. The change of the

dune aspect of the dunes was closely related to the sand-moving wind environment during the observation period. The change of the dune aspect was mainly concentrated near the ridgeline, which was consistent with the erosion area of the dune. However, the analysis of the slope changes showed that the slope proportion of Dune 1 change from November 2015 to April 2016 was greater than that from April 2016 to November 2016. Meanwhile, the slope proportion of the Dune 2 change from November 2015 to April 2016 was smaller than that from April 2016 to November 2016. The reason for this finding was the influence of regional topography, that is, there were many small dunes around Dune 2. Although the regional-scale circulation was similar, the terrain was undulating, which led to a low wind energy environment and weak sand transport capacity. Thus, the change of the dune was not obvious.

#### 4.5 Slope angle

According to the previously presented analysis results, during the observation period, the aspect of the dune did not change significantly under the action of wind. However, the slope of the dune surface



changed significantly because of the change of the erosion or deposition status. As shown in Fig. 8, from November 2015 to April 2016, the area proportion of Dune 1 within the range of 10° to 15°, 20° to 25° and >30° decreased from 25.86%, 20.3%, and 13.16% to 21.8%, 15.99%, and 9.45%, respectively. The total range of slope change was 12.08%, and the range of other slope changes increased. From April 2016 to November 2016, the area proportion of Dune 1 within the range of 10° to 15°, 20° to 25° and >30° increased from 21.8%, 15.99%, and 9.45% to 25.09%, 25.6%, and 15.15%, respectively. The other slope area proportions all reduced, with the total slope change of 18.6%, which was greater than the area change rate during the typical wind season.

Compared with that of Dune 1, the slope of Dune 2 varied slightly both from November 2015 to April 2016 and from April 2016 to November 2016. From November 2015 to April 2016, the area proportion of Dune 2 within the range of 10° to 15°, 20° to 25° and 25° to 30° increased from 17.78%, 22.02%, and 9.27% to 24.08%, 25.5%, and 25.08%, respectively. The total gradient of the slope was 24.98%, and the other slope area proportions all

reduced. From April 2016 to November 2016, the area proportion of Dune 2 within the range of 10° to 15°, 20° to 25°, and 25° to 30° decreased from 24.08%, 25.5%, and 25.08% to 15.29%, 10.23%, and 17.38%, respectively. The total slope change was 31.76%, which was greater than the area change rate from November 2015 to April 2016. The other slope area proportions all reduced.

Notably, whether it was Dune 1 or Dune 2, the sand dune slopes changed considerably under the wind effect. The main area where the slope changed was located on the area where the erosion changed frequently, such as the top of the dune and the sand ridgeline. During the change process of sand dunes, the proportion within the range of 10° to 15°, 20° to 25°, and >30° of Dune 1 and Dune 2 synchronously changed in both the typical wind season and other time. The reason for this conclusion was that the dunes maintained a steady state during the observation period. In addition, the proportion of the area change of the dune from April 2016 to November 2016 was greater than that from November 2015 to April 2016. We observed that there was a correlation between the change of the dune volume during the

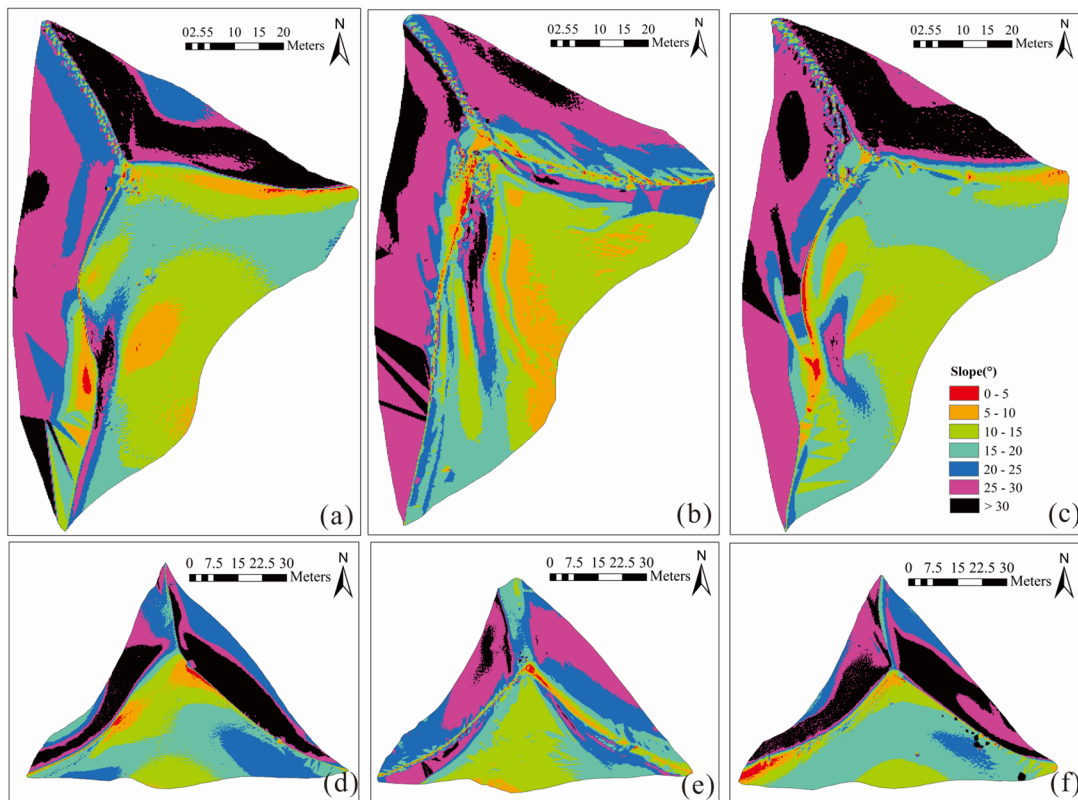


**Fig. 8** Slope of the monitored star dunes in the three monitoring periods. (a) Dune 1 in November 2015; (b) Dune 1 in April 2016; (c) Dune 1 in November 2016; (d) Dune 2 in November 2015; (e) Dune 2 in April 2016; (f) Dune 2 in November 2016.

typical wind season and other time. The amount of volume change during the other time was greater than that during the typical wind season. The larger the variation of the sand dune morphology was, the larger the proportion of the slope changes.

## 5 Discussion

The star dune is one of the tallest sand dunes in the world's sand-sea area. Given its formation in a multi-directional wind environment, the near-surface flow field and sedimentary structure are complex and have a field of aeolian geomorphology. However, in this study, both Dune 1 and Dune 2 formed under three steady wind conditions, although the sand DP was different in 2015, 2016, and 2017. Thus, the slight difference in wind conditions is inadequate to cause the change of sand dune shape, and star dunes of different scales are steady under certain wind conditions. However, the stability degree needs further study. During the growth of the sand dunes, although the height of the sand dunes increases, the volume, length, width, and bottom area of the sand dunes do not increase completely in a positive proportion; it even changes irregularly. Moreover, the variation of sand dune volume during the typical wind season is smaller than the other time. In view of this, we propose two reasons for this phenomenon. The first reason is that the star dunes investigated in this study have not yet developed into mature star dunes; thus, there is still instability between the morphological parameters. The second reason involves the wind condition, sand source, and surrounding terrain environment. When the sand source is insufficient and the wind power is strong, the dune output is more than the dune input in unit time. When the height of the dune increases, the volume of the dune decreases.

The regular dune erosion and deposition are closely related to the regional wind conditions and the sand dunes themselves, such as the shape of dune and the length and direction of dune ridge. The specific performance was that under the influence of wind, and the windward slope of the dune was eroded. But due to the influence of the dune ridge, the airflow separated near the top of sand dune. And then they crossed the ridgeline to the other slopes along the left and right sides. When the wind was strong, the particles could be transported farther and reached the

middle and lower parts of the leeward slope. When the wind was weak, the particles stopped near the ridgeline and collapsed under the action of gravity. However, due to the complex surface airflow of the star dunes, the main wind direction, the angle of the ridgeline, wind strength, and the length and direction of ridgeline could have an impact on the erosion of the dune slope.

We analyzed the degree of the slope change of the star dune during the typical wind season and other time. The distribution of erosion and deposition confirmed that the change of the aspect direction was closely related to the regional wind conditions and dune erosion. However, the variation of the typical wind season was smaller than that of the other time. We determined that slope change was affected by the wind force and dune volume. The larger the volume change of the sand dune was, the greater the change of dune slope. The reason for this finding was that, during the change process, when the wind was strong enough, the sand could climb over the sand ridgeline to reach the leeward slope. Thus, the area of the slip face increased. However, the area within the 20° to 30° slope which was located on the upper part of the windward slope decreased. The sand dunes within this range became the sand source and cross the ridgelines under the wind. Although the height of the sand dunes increased, the volume of the sand dunes decreased. When the wind was not strong enough, the sand could not cross the dune ridgeline. Given that the start-up wind speed of sand within the range of 10° to 20° was slow, the sand accumulates on the top of the dune. And the area ratio within the range of 10° to 20° decreases. During the movement of sand dunes, the kinetic energy of the sand dunes transformed into potential energy. The movement speed of the sand particles decreased. The kinetic energy during the movement of sand dunes was inadequate to maintain the conversion and consumption of the potential energy, so the slope stayed within the range of 20° to 30°. The proportion of the area within the range increased. The height and volume of the dunes increased. Another question was that from November 2015 to April 2016, the area proportion of the Dune 2 within the range of 25° to 30° increased from 9.27% to 25.08%, which was a huge change. But the Dune 2 maintained a steady state. This was another evidence for the steadiness of star dune.

According to the previous study, small-scale dunes were formed by destabilization of sand bed

with a wavelength determined by the sand transport saturation length. The length of wavelength was a few tens of meters (Elbelrhiti et al. 2005). The growth of aeolian giant dunes was affected by the atmospheric boundary layer. The atmospheric boundary layer caused small-scale dunes to superimpose and formed the giant dunes (Andreotti et al. 2002). But in our study, the authors monitored two small-scale star dunes and found the growth rate was very low. There are many giant star dunes near our study area. So according to the results of Andreotti (2002), the small-scale star dune maybe at the initial stages of their development and was expected to grow until they will interact the atmospheric boundary layer. But until now they have not changed significantly even keep their infancy. Our studies prove the possibility of the star dune changing into star sand hills. But this process requires a long time and during this period, the wind conditions in the area cannot change drastically. Therefore, in the later research, the authors will pay more attention to the conditions and factors which can cause the initial stages into giant dunes and then define the key factor.

## 6 Conclusion

1) There are three groups of winds in the study area, namely, northwest, northeast, and south winds. Although the annual sand drift potentials of the three groups of winds are slightly different, the wind direction is basically steady. Notably, the star dunes are formed by a group of relatively steady winds, which confirms the results of previous research. But the differences lie in the huge change of the aspect and slope changed hugely. So the stability of star dune is not complete and it is in a dynamic process.

2) With the increase of the height of the star dunes, the morphological parameters, such as the volume and bottom area, of the dune do not show regular changes.

3) The results of our study showed that the height of the pyramid dunes increases during the typical wind season, but the volume decreases. The height of the sand dunes increases during the other time, but the volume of dune increases. The larger the volume of the dune is, the smaller the change of star dune.

4) The surface erosion during the observation period is closely related to the regional wind conditions for both Dune 1 and Dune 2. However, the

change of the dunes is affected by the wind condition. The sand source also determines the change of the volume and shape of the dune.

5) The larger the star dune is, the slower the increase speed, and the smaller the volume, bottom area, and the moving speed under the same wind conditions, indicating that the scale of the dune is proportional to its stability. The larger the size of the dune, the more stable the dune.

6) The research results showed that the growth process of the star dunes should be this: When the wind was strong, the sand particles would transport from the windward slope to the leeward slope under the action of the wind. The volume the star dune decreases, But the height of star dune increased without enough sand supply. When the wind was weak, the sand moved from surrounding to the top of the dune under the action of the wind. Not only the height of the sand dune increases, but also the volume of the sand dune increases.

7) During the growth of the star dunes, although the slope direction of the sand dunes changes, the overall trend is steady. Moreover, the dune shape maintains its stability during the growth process. The variation of the slope direction during the observation period is closely related to the regional wind conditions and dune erosion.

8) The slope ratio of the sand dunes changes during its growth process, but the overall trend is steady. The stability of the star dunes is verified. Nevertheless, the variation range of the dune slope is proportional to the volume change of the dune. The volume and slope of the sand dunes vary considerably.

## Acknowledgments

This research was supported by the National Key Research and Development Program of China (Grant No.2020YFA0608403-1), the National Natural Science Foundation of China (Grant No. 41871016), the Opening Research Foundation of the Key Laboratory of Desert and Desertification, CAS (KLDD-2020-015), and the Science and Technology Research Project of China Railway First Survey and Design Institute Group Co., Ltd. (2019-10).

We are grateful to Zhao Xueru and Wang Xiaobo for their technical assistance during the survey. Special thanks go to the reviewers and the editors for their helpful comments that have greatly improved the manuscript.

## References

- AN ZS, Zhang KC, Niu QH, et al. (2016) Short-term Dynamic Change of Mega-dunes around the Crescent Spring in Dunhuang. *Arid Zone Res* 33(5): 981-987. (in Chinese) <https://doi.org/10.13866/j.azr.2016.05.10>
- An ZS, Zhang KC, Tan LH, et al. (2018) Dune dynamics in the southern edge of dunhuang oasis and implications for the oasis protection. *J Mt Sci* 15(10): 2172-2181. <https://doi.org/CNKI:SUN:SDKB.o.2018-10-007>
- Andreotti B, Claudin P, Douady S (2002) Selection of dune shapes and velocities part 2: a two-dimensional modelling. *Eur Phys J B* 28(3): 341-352. <https://doi.org/10.1140/epjb/e2002-00237-3>
- Bagnold RA (1941) *The physics of wind blown sand and desert dunes*. London: Methuen.
- Blocken B, Hout AVD, Dekker J, et al. (2015) CFD simulation of wind flow over natural complex terrain: case study with validation by field measurements for ria de Ferrol, Galicia, Spain. *J Wind Eng Ind Aerodyn* 147: 43-57. <https://doi.org/10.1016/j.jweia.2015.09.007>
- Breed CS, Grow T (1979) Morphology and distribution of dunes in sand seas observed by remote sensing. US Government Printing Office, Washington, DC, pp. 253-302.
- Delgado-Fernandez I, Jackson DWT, Cooper JAG, et al. (2013) Field characterization of three-dimensional lee-side airflow patterns under offshore winds at a beach-dune system. *J Geophys Res Earth Surf* 118(2): 706-721. <https://doi.org/10.1002/jgrf.20036>
- Dong Z, Zhang Z, Qian G, et al. (2013) Geomorphology of star dunes in the southern Kumtagh Desert, China: control factors and formation. *Environ Earth Sci* 69(1): 267-277. <https://doi.org/10.1007/s12665-012-1954-y>
- Elbelrhiti H, Claudin P, Andreotti B (2005) Field evidence for surface-wave-induced instability of sand dunes. *Nature* 437: 720-723. <https://doi.org/10.1038/nature04058>
- Fryberger SG, Dean G (1979) *Dune Forms and Wind Regime, A Study of Global Sand Seas*. U.S. Government Printing Office, Washington D.C. pp 137-169.
- Hanke KM, Moser RJII, Rampold P (2015) Historic photos and TLS data fusion for the 3D reconstruction of a monastery altar ensemble. *Remote Sensing Spat. Info. Sci* XL-5/W7, 201-206. <https://doi.org/10.5194/isprsarchives-XL-5-W7-201-2015>
- Isa MA, Lazoglu I (2017) Design and analysis of a 3d laser scanner. *Measurement* 111: 122-133. <https://doi.org/10.1016/j.measurement.2017.07.028>
- Jackson D, Cruz-Avero N, Smyth T, et al. (2013) 3D airflow modelling and dune migration patterns in an arid coastal dune field. *J Coast Res* 65(sp2): 1301-1306. <https://doi.org/10.2112/SI65-220.1>
- Lancaster N (2010) The dynamics of star dunes: an example from the gran desierto, Mexico. *Sedimentology* 36(2): 273-289. <https://doi.org/10.1111/j.1365-3091.1989.tb00607.x>
- Lancaster N (1989) Star dunes. *Prog Phys Geogr* 13(1): 67-91. <https://doi.org/10.1177/030913338901300105>
- Leng Y, Yong Y, Ouyang J, et al. (2006) 3D laser scan for terrain survey in model Yellow River. *Proceedings of SPIE* 6344(1): 634434-6. <https://doi.org/10.1117/12.694437>
- Qu J, Ling Y, Zhang W, et al. (1992) Preliminary observation and study on the formation mechanism of star dune. *J Desert Res* 12(4): 20-28. (In Chinese) <https://doi.org/10.7522/j.issn.1000-694X.2021.00182>
- Rubin DM, Tsoar H, Blumberg DG (2008) A second look at western Sinai seif dunes and their lateral migration. *Geomorphology* 93(3-4): 335-342. <https://doi.org/10.1016/j.geomorph.2007.03.004>
- Tan LH, Zhang WM, Bian K, et al. (2016) Numerical simulation of three-dimensional wind flow patterns over a star dune. *J Wind Eng Ind Aerodyn* 159(7): 1-8. <https://doi.org/10.1016/j.jweia.2016.10.005>
- Ulrike Rösner (1999) Aeolian geomorphology. An introduction. *J Quaternary Sci* 14(1). [https://doi.org/10.1002/\(SICI\)1099-1417\(199902\)14:1<97::AID-JQS368>3.0.CO;2-Y](https://doi.org/10.1002/(SICI)1099-1417(199902)14:1<97::AID-JQS368>3.0.CO;2-Y)
- Wang T, Zhang W, Dong Z, et al. (2005) The dynamic characteristics and migration of a pyramid dune. *Sedimentology* 52(3): 429-440. <https://doi.org/10.1111/j.1365-3091.2005.00696.x>
- Wasson RJ, Hyde R (1984) Factors determining desert dune type (reply). *Nature* 309: 92. <https://doi.org/10.1038/309092a0>
- Xu SY, Xu DF (1983) A primary observation of aeolian sand deposits on eastern shore of the Qinghai Lake. *J Desert Res* 3(3): 11-17. (In Chinese)
- Zhang D, Narteau C, Rozier O, et al. (2012) Morphology and dynamics of star dunes from numerical modelling. *Nature Geosci* 5(7): 463-467. <https://doi.org/10.1038/ngeo1503>
- Zhang WM, Qu JJ, Dong ZB, et al. (2000) The airflow field and dynamic processes of pyramid dunes. *J Arid Environ* 45(4): 357-368. <https://doi.org/10.1006/jare.2000.0643>
- Zhang WM, Qu JJ, Tan LH, et al. (2016) Environmental dynamics of a star dune. *Geomorphology* 27(3): 28-38. <https://doi.org/10.1016/j.geomorph.2016.08.005>
- Zhu Z, Chen Z, Wu Z (1981) *Study on Aeolian Sand Landforms of Taklimakan Desert*. Science Press, Beijing. (In Chinese)